Elevator Abnormal State Detection Based on Vibration Analysis and IF Algorithm

Zhaoxiu Wang
Department of Electronics and Information, Zhangzhou Institute of Technology, Zhangzhou, 363000, China

***Abstract*—Elevators play a crucial role in daily life, and their safety directly impacts the personal and property safety of users. To detect abnormal states of elevators and ensure people's personal safety, the acceleration signal of elevators is decomposed and Weiszfeld algorithm is used to estimate gravity acceleration. In addition, the study also introduces Kalman filtering to reduce error accumulation. To estimate the operating position of elevators, a method based on information fusion is studied and designed to construct a mapping relationship between elevator vibration energy and position, and to locate the height of elevator faults. Finally, an anomaly detection model combining vibration analysis and the Isolated Forest algorithm is developed. The results showed that the main distribution range of acceleration values in the horizontal direction was between 0.02 m^2/s and -0.02 m^2/s. The average estimation error and root mean square error of the research designed elevator position estimation method were 0.109 m and 0.113 m, respectively, which could solve the problem of accumulated position errors. The abnormal vibration energy and height corresponding to different operating conditions of elevators were different. The normal value ratios of the anomaly detection model under different sliding windows were 99.91% and 99.57%, respectively. The anomaly detection model designed for research has good performance and can provide technical support for the detection of elevator operation status.**

***Keywords*—Vibration analysis; IF algorithm; elevator; abnormal; detection**

I. INTRODUCTION

As a vertical transportation tool, elevators are used in various places in daily life, such as office buildings, residences, hotels, large libraries, and industrial and mining enterprises [1]. Elevators are frequently used in people's daily lives, and once any elevator malfunctions, it can pose a serious threat to people's safety. Therefore, timely and accurate detection of elevator abnormal states is crucial. The commonly used methods for elevator status detection include grey prediction model, genetic algorithm, and particle swarm algorithm [2-3].

Skog I designed a new non-invasive elevator fault detection method and corresponding efficient algorithm for detecting elevator faults. This method modeled the traffic load on the elevator through a non-homogeneous Poisson process and described the process using a generalized linear model. The results showed that the method achieved an accuracy of 0.82 with a recall probability of 0.80 [4]. Oya J R G et al. designed a system based on time-domain reflectometry technology to detect elevator belt faults, and constructed a receiver based on compressive sensing to improve positioning capability. The results showed that this method could recover time-domain sparse signals and effectively detect elevator belt faults [5]. Ippili S et al. constructed a one-dimensional convolutional neural network based on sound signals for early identification of faults in rotating machinery, and used this network to process the original time signals. The results showed that this method had good performance in the early identification of rotating machinery faults, and its performance was significantly better than the accelerometer based method [6]. Mian T et al. designed a multi-sensor fault diagnosis system based on infrared thermal imaging and vibration sensors for diagnosing faults in rotating machines. In addition, the study also utilized deep convolutional neural networks, support vector machines, and principal component analysis. The results showed that this method could effectively diagnose faults in rotating machines under all working conditions [7].

However, these methods also have certain issues, such as the stronger dependence of model-based methods on specific parameters of elevator systems compared to data-driven methods on data training. To detect abnormal states in elevators, an anomaly detection model based on vibration analysis of horizontal vibration signals and Isolation Forest (IF) algorithm is designed. Methods are also designed to reduce the accumulation of position errors and estimate elevator dynamic characteristics. The research aims to improve the accuracy of elevator anomaly detection, avoid serious elevator accidents, and ensure people's personal safety. The innovation of the research is reflected in the combination of vibration analysis and IF algorithm, which reduces the cumulative position error and improves the efficiency of elevator anomaly detection. To better demonstrate the advantages of the design method proposed in this article, the study will compare it with existing methods in terms of performance indicators, scalability, and limitations. The comparison results are shown in Table I.

TABLE I. COMPARISON WITH RELATED WORK

Serial number	Performance index		Scalability	Limitation
	F1	Accuracy		
[4]	0.800	0.820	F1 drops to 0.685 on larger datasets	Model complexity and difficulty in parameter estimation
[5]	0.847	0.886	When facing multiple types of elevator belts, a significant amount of customized training is required	Limited measurement accuracy and signal quality issues
[6]	0.929	0.936	Cannot be compatible with new data types	Insufficient utilization of sequence order information
[7]	0.935	0.941	Difficulty in expanding sensor types	Easy overfitting and high computational resource consumption
Manuscript	0.988	0.992	Low cost, strong universality and scalability	Not much consideration has been given to the fault detection of elevator door systems

II. METHODS AND MATERIALS

To detect abnormal states in elevators, an anomaly detection method based on vibration analysis and IF algorithm is studied and designed. Due to the use of horizontal acceleration signals for anomaly detection, the study also designs a method for estimating elevator gravity acceleration and dynamic characteristics. In addition, the study also designs a method for estimating the operating position of elevators.

A. Design of Estimation Method for Elevator Gravity Acceleration and Dynamic Characteristics

To detect abnormal states in elevators, a gravity acceleration and dynamic feature estimation method is first designed to reduce error accumulation and improve detection accuracy. Secondly, a method for estimating the operating position of elevators is studied and designed to facilitate the construction of the mapping relationship between elevator vibration energy and position in the future. Finally, an anomaly detection method based on vibration analysis and IF algorithm is studied and designed. The study uses a three-axis acceleration sensor (MPU6050) to collect three-dimensional acceleration signals from the elevator, and decomposes the acceleration three-dimensional vector based on the gravity acceleration vector calibrated by the sensor. After that, the components in the direction of gravity acceleration can be obtained. The Weiszfeld algorithm is adopted for the estimation of elevator gravity acceleration. The Weiszfeld algorithm is a classic iterative algorithm for solving single facility site selection problems, which can obtain the optimal solution of the problem, and the essence of this algorithm is a steepest descent method. The Weiszfeld algorithm, as a repeated weighted least squares method, has the advantage of being able to handle weighted point sets and gradually converge to the optimal solution during the iteration process [8-9]. In addition, unlike some methods that rely on specific prior knowledge or assumptions, the Weiszfeld algorithm does not require extensive knowledge of the elevator's operating status, system parameters, etc. when estimating elevator gravity acceleration, and has a wider applicability [10-11]. The solution for this algorithm is shown in Eq. (1).

$$\begin{cases} x_{k+1} = \sum_{i=1}^{a} \frac{b_i}{E_i(x_k, y_k, z_k)} \div \sum_{i=1}^{a} \frac{1}{E_i(x_k, y_k, z_k)} \\ y_{k+1} = \sum_{i=1}^{a} \frac{c_i}{E_i(x_k, y_k, z_k)} \div \sum_{i=1}^{a} \frac{1}{E_i(x_k, y_k, z_k)} \\ z_{k+1} = \sum_{i=1}^{a} \frac{d_i}{E_i(x_k, y_k, z_k)} \div \sum_{i=1}^{a} \frac{1}{E_i(x_k, y_k, z_k)} \end{cases} \quad (1)$$

In Eq. (1), (x_k, y_k, z_k) represents the median center solved by Weiszfeld algorithm after the k th iteration, and x, y, and z are vectors on the x-axis, y-axis, and z-axis, respectively. a represents the number of measured gravitational acceleration vectors, and (b_i, c_i, d_i) is the gravitational acceleration vector obtained from the i measurement. $E_i(x_k, y_k, z_k)$ represents the distance between (b_i, c_i, d_i) and the median center obtained from the k iteration. $(x_{k+1}, y_{k+1}, z_{k+1})$ represents the new median center. The calculation of $E_i(x_k, y_k, z_k)$ is shown in Eq. (2).

$$E_i(x_k, y_k, z_k) = \left\| (b_i, c_i, d_i) - (x_k, y_k, z_k) \right\| \quad (2)$$

The operation process of an elevator can be mainly divided into four states: stationary, accelerating, uniform, and decelerating, and the acceleration in all four ideal states remains constant [12]. To estimate the kinematic characteristics of elevators, the Kalman filtering method is used in the study. The advantage of the Kalman filtering method is that it can update the state estimation based on previous estimates and current measurements, and has strong robustness and adaptability [13-14]. The representation of elevator dynamic characteristics is shown in Eq. (3).

$$\chi_k = F_k \chi_{k-1} + \omega_k \quad (3)$$

In Eq. (3), χ_k represents the system state vector, F_k represents the state transition function, and ω_k represents the process noise vector. The expression of χ_k is shown in Eq. (4).

$$x_k \triangleq \begin{bmatrix} x'_k \\ x''_k \\ x'''_k \end{bmatrix} \quad (4)$$

In Eq. (4), $\triangleq$represents the identity equation, while χ'_k, χ''_k, and χ'''_k represent velocity, acceleration, and jerk, respectively. The expression of F_k is shown in Eq. (5).

$$F_k \triangleq \begin{bmatrix} 1 & g & \frac{g^2}{2} \\ & 1 & g \\ & & 1 \end{bmatrix} \quad (5)$$

In Eq. (5), g represents the sampling time interval. To output the system state vector, the Kalman filtering method

needs to perform optimal estimation based on the prediction step and update step. Optimization estimation mainly includes four steps. The first step is to solve g and adjust F_k and process noise covariance Q_k based on g. The second step is to predict the state of the next time step and estimate the system covariance $\bar{P}_k$. The third step is to solve the Kalman gain K_k, and the fourth step is to solve the novel Y_k. The fifth step is to adjust the state prediction value and prediction covariance, and refresh the system state. The processing of the covariance matrix P_k is shown in Eq. (6).

$$P_k = (I - K_k H_k) \times \bar{P}_k \times (I - K_k H_k)^T + K_k R_k \times K_k^T \quad (6)$$

In Eq. (6), I is the identity matrix, H_k represents the measurement function, and R_k represents the observed noise variance. Since the measured values of acceleration sensors during elevator operations are typically non-zero, threshold values and corresponding constraints are introduced in the study. The automatic correction process of gravity acceleration is shown in Fig. 1.

From Fig. 1, the automatic correction process of gravity acceleration mainly consists of six steps. The first step is to determine whether the elevator is stationary. If it is stationary, slide the window to collect data, otherwise the process ends. The second step is to filter out outliers, and the third step is to use the Weiszfeld algorithm. The fourth step is to update the gravitational acceleration, and the fifth step is to determine whether the elevator is moving. If it is running, the process ends; otherwise, the sliding window continues to collect data.

B. Design of Elevator Operation Position Estimation Method

To locate the operating position of the elevator, the study first models the elevator floor information through acceleration sensors and Simultaneous Localization and Mapping (SLAM) algorithm. Secondly, the study uses a pressure sensor to solve the operating height of the elevator. Finally, a method for estimating the operating position of elevators based on information fusion is studied and designed. The elevator displacement solved by acceleration sensors has the advantage of high short-term accuracy, but there is also a drawback of fast error accumulation. Therefore, the SLAM algorithm is introduced to compensate for this deficiency. The advantage of the SLAM algorithm is its ability to integrate multiple sources of information and incorporate Kalman filtering technology [15]. By using the Kalman filter in the SLAM algorithm, it is possible to obtain the floor spacing and floor height. The expression for the distance of elevator operation between two stops is shown in Eq. (7).

$$S_k = F_k S_{k-1} + B_k u_k + \omega_k \quad (7)$$

In Eq. (7), u_k is the control vector, B_k is the control matrix, and S_k represents the displacement of the elevator from rest. The expression of B_k is shown in Eq. (8).

$$B_k = \left(g, \frac{g^2}{2} \right) \quad (8)$$

The initialization process of elevator floor information mainly consists of seven steps, including acceleration data collection, elevator motion judgment, calculation of elevator displacement and displacement error, judgment of whether the elevator is going up, judgment of whether the elevator is stationary, updating map information, and judgment of whether the set number of times has been reached. To solve the operating height of the elevator, a pressure sensor is used in the study. The advantage of air pressure sensors is that they can directly obtain real-time altitude information of elevators, and the error accumulation is slow [16-17]. The difference γ between the starting and measuring heights is solved as shown in Eq. (9).

$$\gamma = \left(\frac{JL}{WN} \right) \ln \left(\frac{\rho_0}{\rho} \right) \quad (9)$$

In Eq. (9), ρ_0 and ρ represent the atmospheric pressure at the starting and measuring heights, respectively, and N represents the molar mass of air. J represents the universal gas constant, L represents the measured air temperature, and W represents the gravitational acceleration of the Earth's surface. The solution for the current altitude ϕ is shown in Eq. (10) [18-19].

$$\phi = 44330 \times \left(1 - \left(\frac{\rho}{\rho_0} \right)^{\frac{1}{5.255}} \right) \quad (10)$$

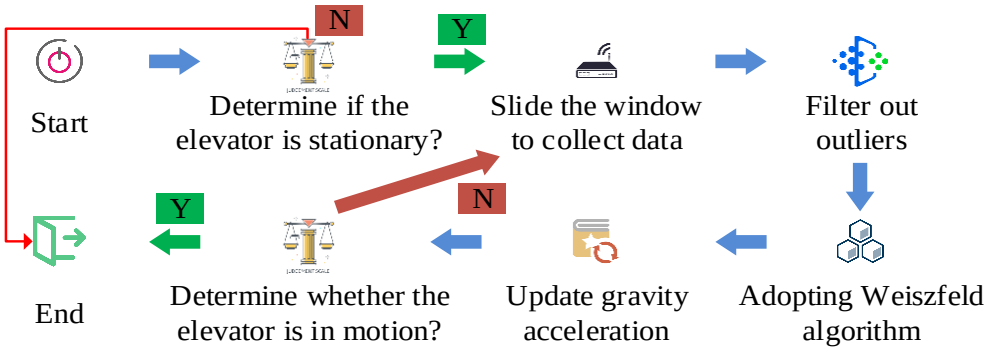

Fig. 1. Automatic correction process of gravity acceleration.

The solution of γ can be simplified as shown in Eq. (11).

$$\gamma = \phi - \phi_0 \tag{11}$$

In Eq. (11), ϕ_0 represents the altitude of the reference position. To preprocess the obtained height data and reduce the impact of noise, a first-order exponential smoothing method is used in the study. The advantage of this method is that it makes extrapolation predictions more realistic and has high practicality and effectiveness in time series prediction [20]. The current time step estimation value η_t is solved as shown in Eq. (12).

$$\eta_t = \beta\sigma_t + (1-\beta)\eta_{t-1} \tag{12}$$

In Eq. (12), η_{t-1} represents the estimated value of the previous time step, β represents the smoothing coefficient, and $\beta \in (0,1)$ and σ_t are the measured values of the current time step. t stands for Time. To estimate the operating position of the elevator, a combination of acceleration sensors and air pressure sensors is studied, and floor information is also introduced. Unscented Kalman Filter (UKF) is used to apply this information. Therefore, the solution for the operating height θ_τ of the elevator at τ time is shown in Eq. (13).

$$\theta_\tau = \theta_{\tau-1} + B_k u_k + \omega_k \tag{13}$$

The state transition function of the elevator system is expressed as Eq. (14).

$$\theta_\tau = f(\theta_{\tau-1}) = \begin{cases} \theta_{\tau-1} + B_k u_k + \omega_k & \text{Motion} \\ f\theta_j \quad \theta_{\tau-1} \in U\left(f\theta_j, \delta_{f\theta_j}\right) & \text{Static} \end{cases} \tag{14}$$

In Eq. (14), $f\theta_j$ represents the height of the car relative to the reference point, j is the number of heights, U is the symbol for the set, and $\delta_{f\theta_j}$ represents the prior measurement error. The core of UKF is the traceless transformation, as shown in Fig. 2.

In Fig. 2, ϑ represents a set of sigma points, and ψ represents a new set of points after nonlinear changes. The green and orange dots in the blue background represent the mean and covariance of the transformation point set, respectively, and are considered as new predicted values. To select sigma points, a symmetric sampling strategy is adopted in the study. The elevator position tracking process based on UKF is shown in Fig. 3.

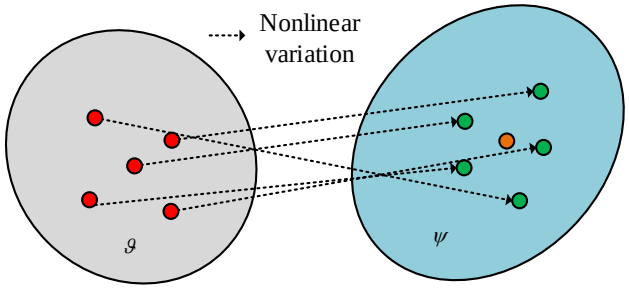

Fig. 2. Diagram of unscented transformation.

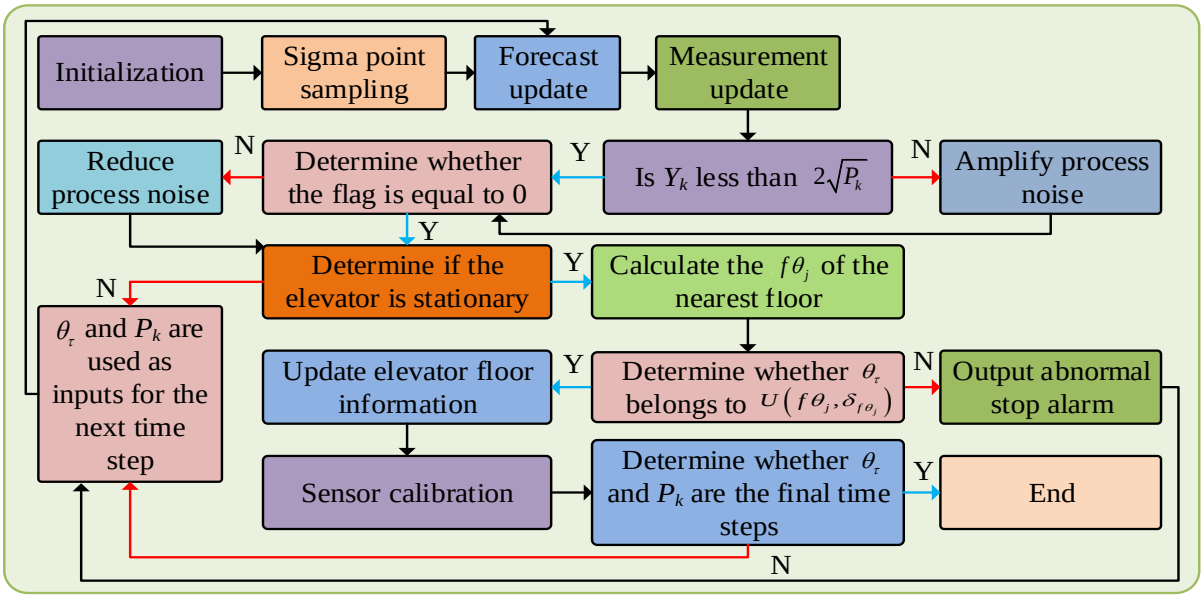

Fig. 3. Elevator position tracking process based on UKF.

From Fig. 3, the first step of the elevator position tracking process based on UKF is initialization, and the second step is sigma point sampling. The third step is to predict updates, and the fourth step is to measure updates. The fifth step is to determine whether Y_k is smaller than $2\sqrt{P_k}$. If it is less than, proceed to step six; otherwise, amplify the process noise before proceeding to step six. The sixth step is to determine whether the flag is equal to 0. If it is equal, proceed to step seven; otherwise, reduce the process noise before proceeding to step seven. The seventh step is to determine whether the elevator is

stationary. If it is stationary, calculate the $f\theta_j$ of the nearest floor. Otherwise, use it as input for the next time step of θ_τ and P_k. The eighth step is to determine whether θ_τ belongs to $U\left(f\theta_j, \delta_{f\theta_j}\right)$. If it belongs, update the elevator floor information. Otherwise, output an abnormal stop alarm. The ninth step is to perform sensor calibration, and the tenth step is to determine whether θ_τ and P_k are the final time steps. If so, the process ends. Otherwise, θ_τ and P_k are inputted for the next time step, and then return to the second step.

C. Design of Elevator Abnormal State Detection Method

To detect abnormal states in elevators, the study first constructs a mapping of elevator vibration energy and position based on vibration analysis. Secondly, the study uses the IF algorithm to train the elevator anomaly detection model. To determine the operating status of the elevator, the study considers the vibration of the elevator car as an important feature. To determine whether the data is abnormal, a baseline is constructed for elevator normal operation. In addition, the study uses horizontal acceleration signals to detect abnormal vibrations. The steps of the baseline generation method are shown in Fig. 4.

From Fig. 4, the first step in baseline generation is data collection, and the second step is to determine whether the baseline has been generated. If it has been generated, end the process; otherwise, perform data preprocessing and feature extraction. The third step is to obtain horizontal vibration energy, and the fourth step is to obtain cluster data. The fifth step is to calculate the moving average, and the sixth step is to calculate the moving average error. The seventh step is to determine whether the slope of the moving average error is approximately equal to 0. If it is, a baseline is generated and the process ends. Otherwise, the process returns to the first step. The solution for the moving average MA_n is shown in Eq. (15) [21].

$$MA_n = \frac{\sum_{r=1}^{n} |\Pi_r|^2}{n} \tag{15}$$

In Eq. (15), n represents the number of collected signals, Π_r represents the root mean square of the r horizontal vibration signal, and r is the signal number. To clarify the abnormal state of the elevator, the intrinsic feature scale decomposition method is used to decompose the horizontal vibration signal, and envelope spectrum analysis is used to detect the impact signal to eliminate false alarms. To suppress the endpoint effect, the method of mirror extension is used in the study. To construct a mapping between elevator vibration energy and position to detect the vibration state of the guide rail on the highest and lowest floors, a horizontal acceleration signal is used and solved using the established elevator acceleration and position estimation method. To further detect outliers, the study adopts the IF algorithm and trains the outlier detection model through the IF algorithm. The IF algorithm, as an unsupervised method, has the advantages of low computational cost, linear time complexity, and does not rely on abnormal samples [22]. In addition, compared with similar outlier detection methods, the IF algorithm does not require calculating the distance or density between data points like some distance or density-based methods, has lower time complexity, and does not rely on data distribution assumptions. It is relatively insensitive to noise and outliers in the data, and can effectively identify true outliers, making it less susceptible to noise interference and misjudgment [23-24]. The IF algorithm uses the idea of ensemble learning and requires the construction of isolated trees. The construction process of an isolated tree is shown in Fig. 5.

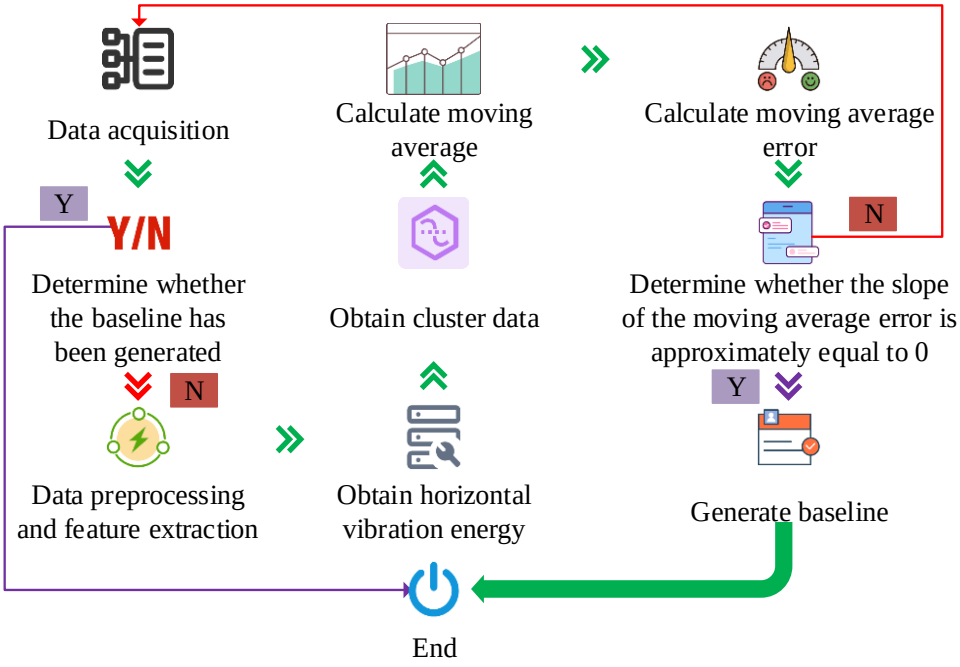

Fig. 4. Steps of baseline generation method.

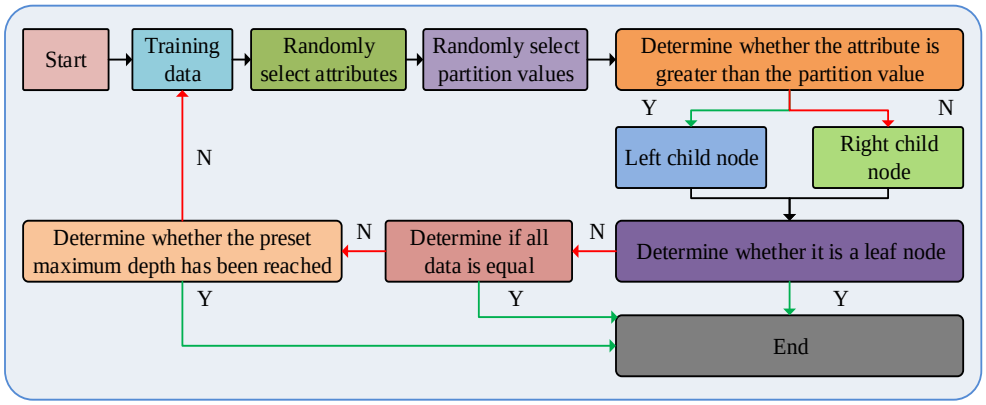

Fig. 5. The construction process of isolated trees.

From Fig. 5, the first step in constructing an isolated tree is to train the data, and the second step is to randomly select the attribute ε. The third step is to randomly select the partition value μ, and the fourth step is to determine whether ε is greater than μ. If it is judged as yes, place it in the left child node; otherwise, place it in the right child node. The fifth step is to determine whether it is a leaf node. If it is, the process ends; otherwise, the next step is to proceed. The sixth step is to determine whether all data are equal. If they are equal, the process ends; otherwise, it enters the seventh step. The seventh step is to determine whether the preset maximum depth has been reached. If it has been reached, the process ends. Otherwise, it returns to the first step and repeats the process until it ends. The process of elevator anomaly detection method based on vibration analysis and IF algorithm is shown in Fig. 6.

From Fig. 6, the first step of the elevator anomaly detection method is to collect acceleration signals, and the second step is to estimate the elevator position. The third step is to establish a baseline, and the fourth step is envelope spectrum analysis. The fifth step is to generate data records, and the sixth step is to determine whether the sliding window is full. If it is full, the detection model is used for anomaly detection. Otherwise, the process returns to the fifth step. The seventh step is to determine if the anomaly rate is too high. If it is too high, an alarm will be triggered and the process will end. Otherwise, the data will be added to the buffer. The eighth step is to determine whether the number of records is greater than the set threshold. If it is, the detection model will be retrained based on the training data. Otherwise, it will return to the data buffer.

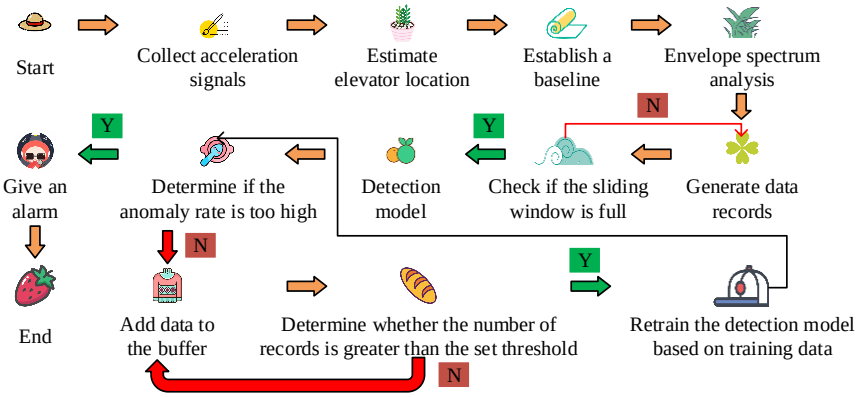

Fig. 6. The process of elevator anomaly detection method based on vibration analysis and IF algorithm.

III. Results

To analyze the detection results of elevator abnormal states, the study explained the experimental data collection equipment, experimental environment, and other experimental devices, and analyzed the results of acceleration information decomposition. Afterwards, the study analyzed the results of elevator position tracking and constructed the relationship between elevator vibration energy and position mapping. Finally, the study validated the performance of the IF model in detecting elevator abnormal states.

A. Acceleration Information Decomposition and Motion Feature Estimation Results

To collect elevator data, the study used Raspberry Pi 4B and added MPU6050 acceleration sensor, BMP180 air pressure sensor, and touch switch. The experimental environment used was the elevator in the experimental building. The operating system used in the experiment was Raspbian, the built-in operating system of Raspberry Pi. The processor was Broadcom BCM2711, with a clock speed of 1.5GHz, a maximum supported memory capacity of 4GB, and a thermal design power consumption of 7.5W. The collected signal would be decomposed, and the decomposition result is shown in Fig.

7.

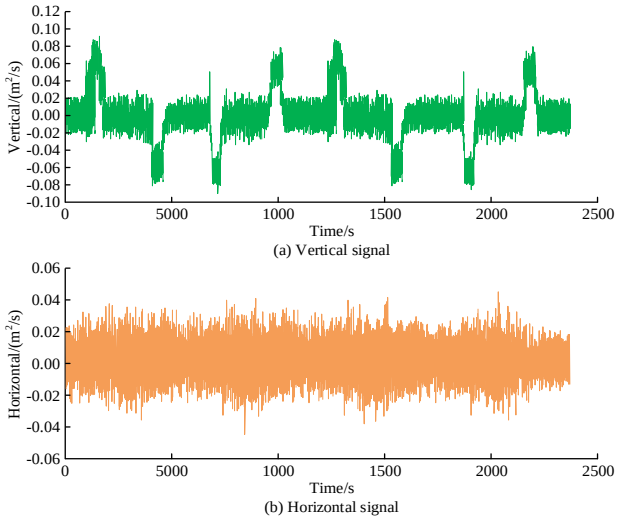

Fig. 7. The result of signal decomposition.

In information decomposition, the study first collected the residual distribution of the acceleration signal minus the calibrated gravity acceleration in three-dimensional space. Secondly, the distribution was decomposed into vertical and horizontal acceleration signals in three-dimensional space, as shown in Fig. 7 (a) and Fig. 7 (b). According to Fig. 7 (a), after decomposing the acceleration information, the maximum and minimum vertical acceleration values were 0.09375 m^2/s and -0.09063 m^2/s, respectively. As time increased, the vertical acceleration value exhibited a fluctuating trend of gentle, upward, and downward fluctuations. According to Fig. 7 (b), in the horizontal direction, the maximum acceleration value was 0.0450 m^2/s and the minimum value was -0.0457 m^2/s. As time gradually increased, the horizontal acceleration value exhibited a fluctuating upward and downward trend. In addition, the main distribution range of acceleration values in the horizontal direction was between 0.02 m^2/s and -0.02 m^2/s. Through signal decomposition, three-dimensional data can be transformed into one-dimensional data. This not only facilitates the installation of sensors, but also enhances the robustness of the system. The analysis of motion characteristics is shown in Fig. 8.

According to Fig. 8 (a), in terms of acceleration characteristics, the maximum and minimum values of the source data were 1.0 m^2/s and -0.75 m^2/s, respectively. The maximum and minimum values of the filtered data's maximum acceleration were 0.71 m^2/s and -0.72 m^2/s, respectively. The maximum and minimum values of the maximum deceleration were 0.76 m^2/s and -0.75 m^2/s, respectively. From Fig. 8 (b), at 95% of the sampled data, the maximum values of acceleration and deceleration were 0.75 m^2/s and 0.68 m^2/s, respectively, with a difference of 0.07 m^2/s between the two. In addition, the minimum acceleration value was -0.74 m^2/s, which differed from the minimum deceleration value of -0.59 m^2/s by 0.15 m^2/s. In Fig. 8 (c), with the increase of time, the elevator speed exhibited a cyclic upward and downward trend. In addition, the maximum and minimum values of the velocity characteristics were 1.81 m^2/s and -1.89 m^2/s, respectively. Both the acceleration and deceleration, as well as the maximum acceleration and deceleration, were within the standard range.

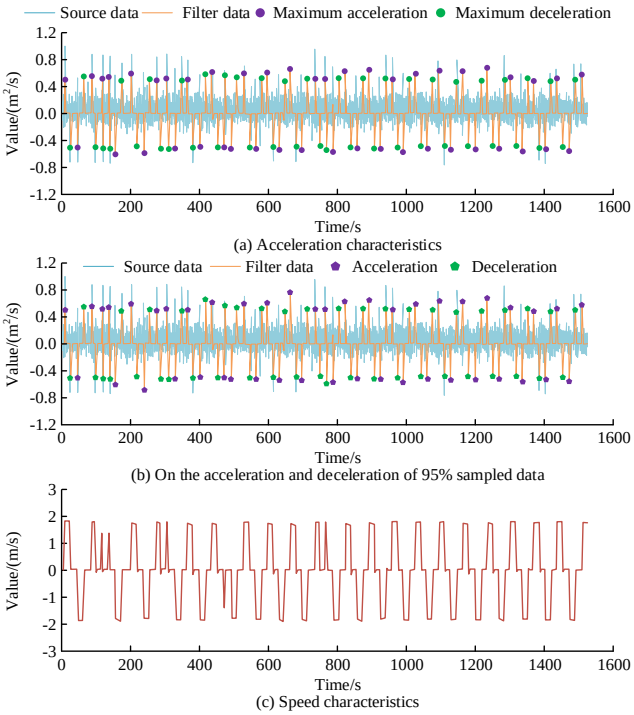

Fig. 8. Analysis of motion characteristics.

B. Analysis of Elevator Position Tracking Results

To track the position of the elevator, the study used the same Raspberry Pi and sensors to collect elevator data. The operating position of the elevator in the experimental building was a total of 8 floors, and the floor height and spacing were generally around 4 meters. The scanning range of SLAM was 0.1-30 meters, with a measurement accuracy of ±2 centimeters, a time interval of 50Hz, and a positioning accuracy of 10 centimeters. The measurement matrix of UKF was 1, the sampling time interval was 0.5s, the process noise covariance was 1, and the measurement noise covariance matrix was 0.01. Based on the collected information from acceleration sensors and air pressure sensors, the study combined these two types of information through UKF and obtained the tracking results and estimation errors of the elevator position, as shown in Figure 9.

From Fig. 9 (a), the maximum value of elevator position using only the UKF method was 31.3m, and the minimum value was -0.8m. The maximum values of elevator position using UKF+automatic calibration method and UKF+ automatic calibration+SLAM method were 29.3m and 28.5m, respectively, with a difference of 0.8m between the two, and the minimum value of elevator position under both methods was 0m. The automatic calibration method and SLAM effectively reduced the errors observed in the UKF method. In Fig. 9 (b), the cumulative probability of errors at different positions varied under different methods. For example, when the position error was 0.5m, the cumulative probabilities of the UKF method, UKF+automatic calibration method, and UKF+automatic calibration+SLAM method were 0.327, 0.684, and 1.00, respectively. In addition, the average estimation errors of the three methods were 0.923m, 0.395m, and 0.109m, respectively, and the root mean square errors were 0.943m, 0.404m, and 0.113m, respectively. The UKF+automatic calibration+SLAM

method had the smallest estimation error, followed by the UKF+ automatic calibration method. In summary, the UKF+automatic calibration+SLAM method can effectively solve the problem of accumulated position errors and accurately track the operating position of elevators.

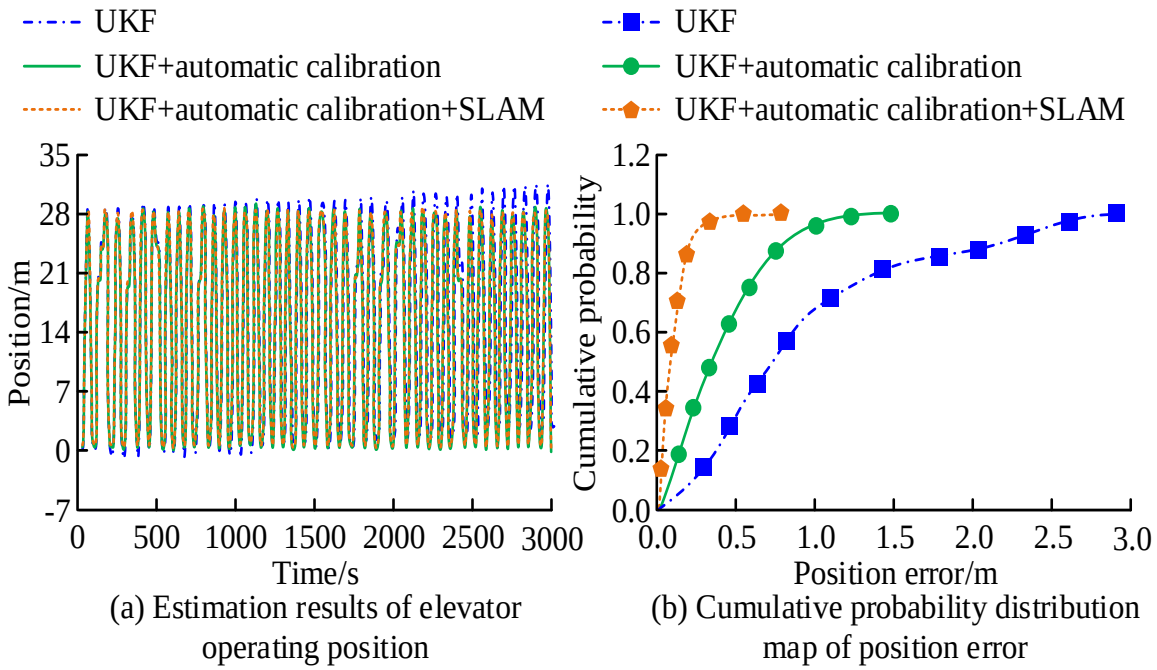

(a) Estimation results of elevator operating position

(b) Cumulative probability distribution map of position error

Fig. 9. Tracking results and estimation errors of elevator position.

C. Analysis of Elevator Abnormal State Detection Results

To detect abnormal states in elevators, the same experimental environment and setup were used in the study. In collecting data, the experiment also used Raspberry Pi and sensors. In the collected baseline data, the sub healthy line was 0.140m/s^2 and the fault line was 0.162m/s^2. In addition, the study also removed useless attributes of the data, such as running time, and only retained the maximum acceleration/deceleration, maximum speed, 95th percentile of acceleration, and 5th percentile of deceleration. The total number of isolated trees was 120, the threshold for outliers was -0.18, the maximum sampling number was 267, and the proportion of outliers in the training data was 99.69%. The width of the sliding window was 800, and the study selected the outlier distribution of the third and ninth windows for analysis. The envelope spectrum analysis was conducted on the first product component of the vibration signal, and the amplitude before and after analysis is shown in Fig. 10.

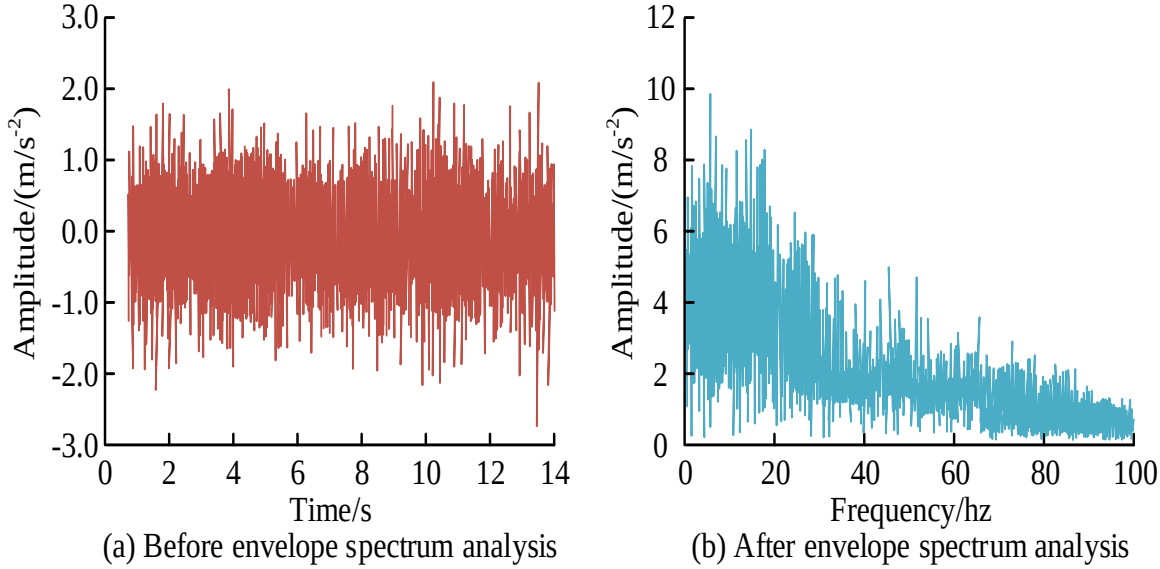

(a) Before envelope spectrum analysis

(b) After envelope spectrum analysis

Fig. 10. The amplitude before and after the envelope spectrum analysis of the first product component.

According to Fig. 10 (a), before demodulating the product component 1, its corresponding amplitude was mainly concentrated between 0.5m/s^{-2} and -0.7m/s^{-2}, and the maximum and minimum amplitudes were 0.208m/s^{-2} and -0.273m/s^{-2}, respectively. As time went by, the vibration kept rising, falling, and fluctuating repeatedly. From Fig. 10 (b), after demodulating the product component 1, as the frequency increased, the vibration gradually decreased, and the range of up and down fluctuations also narrowed. The maximum and minimum amplitude values were 9.98m/s^2 and 0.00m/s^2, respectively. In addition, the vibration energy of the signal was primarily concentrated in the low-frequency range, with fewer high-frequency impulsive signals. This indicated that the outlier was false and consistent with the actual situation. The relationship between elevator vibration energy and position mapping is shown in Fig. 11.

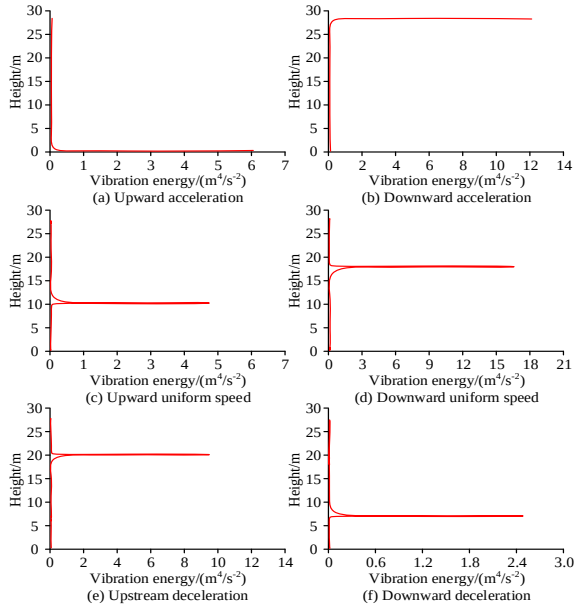

Fig. 11. The relationship between elevator vibration energy and position mapping.

In Fig. 11, the vertical axis represents the operating position of the elevator, and the horizontal axis represents the vibration energy at the corresponding position. The peaks in the spectrum are the abnormal vibrations generated by simulated faults. From Fig. 11 (a), when the elevator accelerated upwards, the abnormal vibration energy generated during the simulated fault was 6.02m4/s^{-2}, and the corresponding height at this time was 0m. From Fig. 11 (b), 11 (c), 11 (d), 11 (e), and 11 (f), peaks appeared during the elevator's downward acceleration, upward uniform speed, downward uniform speed, upward deceleration, and downward deceleration. This indicated that abnormal vibrations occurred in the elevator in all five cases, and the vibration energy and fault height varied in different situations. For example, if the elevator was moving at a constant speed, the abnormal vibration energy corresponding to the up and down directions of the elevator was 4.78m4/s^{-2} and 16.8m4/s^{-2}, respectively, and the corresponding fault heights were 10m and 18m, respectively. It can be seen that the occurrence of simulated faults could be clearly detected at various stages of elevator operation, and the position of the car where the fault occurred, that is, the position where the guide rail may have malfunctioned, could be located, providing important information for the maintenance of the elevator system and the rescue of trapped personnel. The distribution of outliers for different sliding windows is shown in Fig. 12.

In Fig. 12 (a), under the third sliding window, the abnormal scores were mainly concentrated in the range of 0.10 and 0.15. In addition, the proportion of normal values greater than the threshold of -0.18 outliers was approximately 99.91%. According to Fig. 12 (b), in the 9th sliding window, the proportion of normal values greater than the outlier threshold was about 99.57%, and the outlier scored with more than 10 data points were mainly concentrated in the range of 0.067 to 0.15. In addition, the maximum number of outlier data points was 58, corresponding to outlier scores of 0.123 and 0.147. Overall, the IF model could effectively detect the operational status of elevators.

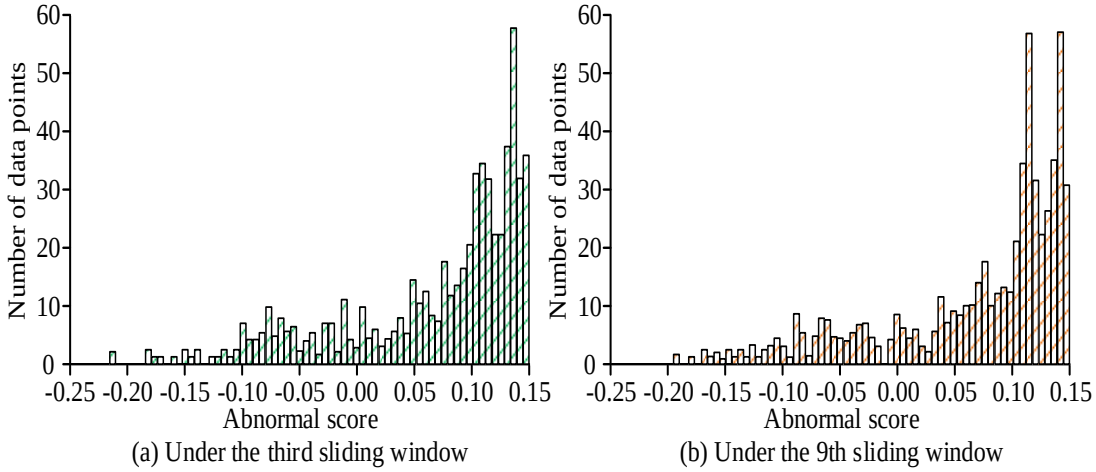

Fig. 12. Outlier distribution of different sliding windows.

IV. Discussion and Conclusion

Aiming at the problem of detecting abnormal states in elevators, a dynamic prediction method for elevators and an information fusion-based elevator operation position tracking method were studied and designed. An anomaly detection model based on vibration analysis and IF algorithm was also constructed. The results showed that after signal decomposition, the maximum acceleration values corresponding to the vertical and horizontal directions were 0.09375 m^2/s and 0.0450 m^2/s, respectively, and the minimum acceleration values were -0.09063 m^2/s and -0.0457 m^2/s, respectively. Signal decomposition could transform three-dimensional data into one-dimensional data, enhancing the robustness of the system. The average estimation errors of UKF method, UKF+automatic calibration method, and UKF+automatic calibration+SLAM method were 0.923m, 0.395m, and 0.109m, respectively, with root mean square errors of 0.943m, 0.404m, and 0.113m, respectively. This indicated that both automatic calibration and SLAM algorithms could to some extent solve the problem of accumulated position errors. The maximum amplitude values of product component 1 before and after demodulation were 0.208m/s^{-2} and 9.98m/s^{-2}, respectively, and the vibration energy of the demodulated signal was mainly concentrated in the low-frequency range, with less high-frequency impulsive signals, which was in line with the actual situation. Under different operating conditions of the elevator, simulated faults had corresponding peak signals, and the vibration energy and height corresponding to the peak signals were also different under different operating conditions. In the third and fifth sliding windows, the proportion of normal values greater than the outlier threshold was 99.91% and 99.57%, respectively. The research designed anomaly detection models had good performance. This method could monitor and analyze the acceleration signals and vibration data of the equipment in real time, predict potential faults, and thus improve safety. It can be applied to elevators in construction sites, mine elevators, rail transit systems, industrial automation equipment, key components in the aerospace industry, lifting systems in marine engineering, as well as medical and emergency rescue equipment, ensuring the stability and safety of these systems during operation, reducing accident risks, and has significant practical application value.

However, there are also certain limitations to the research. Firstly, there was not much consideration given to the fault detection of elevator door systems in research. Technologies such as photosensitive sensors or image-based door anomaly detection are important components in addressing the safety of elevator door systems. Light sensors can monitor the status of elevator doors by sensing light, while image-based door anomaly detection technology requires advanced image processing algorithms and computer vision technology. Secondly, the study used unsupervised IF algorithm. However, relying solely on Unsupervised Learning is difficult to fully explore the deep information of data. Future research can combine Unsupervised Learning and Supervised Learning to further improve the detection accuracy and robustness of the model, especially in the case of labeled datasets. Thirdly, sensor data may be affected by environmental noise, which can affect the accuracy of elevator status monitoring. Future research could consider deep learning techniques to address noise issues, improving noise processing accuracy by learning the features and patterns of noise. Fourthly, although UKF theoretically has high accuracy, it may face computational efficiency challenges in practical applications, especially in scenarios with large data volumes or high real-time requirements. Future research can explore model light weighting to reduce the time and resources required for retraining models on new tasks, as well as reduce the difficulty of model optimization and improve application efficiency through automated joint optimization. Fifthly, the deployment of this method in real environments will face complex building environments, especially large buildings with complex internal structures that may include multiple elevator shafts, different floors, and complex building layouts, leading to interference in sensor signals. Future research can optimize the layout and selection of sensors, reduce space occupation, and choose high-quality sensors. Shielding and filtering techniques can also be used to reduce interference.

References

[1] Nguyen T V, Jeong J H, Jo J. An efficient approach for the elevator button manipulation using the visual-based self-driving mobile manipulator. Industrial Robot: the international journal of robotics research and application, 2023, 50(1):84-93.

[2] Beamurgia M, Basagoiti R, Rodríguez I, Rodríguez V. Improving waiting time and energy consumption performance of a bi-objective genetic algorithm embedded in an elevator group control system through passenger flow estimation. Soft Computing, 2022, 26(24):13673-13692.

[3] Mangera M, Pedro J O, Panday A. GA-optimised nonlinear pseudo-derivative feedback control of a sustainable, high-speed, ultratall building elevator. International Journal of Dynamics and Control, 2022, 10(6):1903-1921.

[4] Skog I. Nonintrusive Elevator System Fault Detection Using Learned Traffic Patterns. IEEE Sensors Letters, 2020, 4(11):1-4.

[5] Oya J R G, Hidalgo-Fort E, Chavero F M, Carvajal R G. Compressive-Sensing-Based Reflectometer for Sparse-Fault Detection in Elevator Belts. IEEE Transactions on Instrumentation and Measurement, 2020, 69(1):947-949.

[6] Ippili S, Russell M B, Herrin W D W. Deep learning-based mechanical fault detection and diagnosis of electric motors using directional characteristics of acoustic signals. Noise Control Engineering Journal, 2023, 71(5):384-389.

[7] Mian T, Choudhary A, Fatima S. Multi-sensor fault diagnosis for misalignment and unbalance detection using machine learning. IEEE Transactions on Industry Applications, 2023, 59(5):5749-5759.

[8] Neumayer S, Nimmer M, Setzer S, Steidl G. On the Robust PCA and Weiszfeld's Algorithm. Applied Mathematics and Optimization, 2020, 82(3):1017-1048.

[9] Groumpos P P. A Critical Historic Overview of Artificial Intelligence: Issues, Challenges, Opportunities, and Threats. Artificial Intelligence and Applications. 2023, 1(4):197-213.

[10] Feng X. Multiplant Location Involving Resource Allocation. GEOGRAPHICAL ANALYSIS, 2024, 56(1):97-117.

[11] Rezova N, Kazakovtsev L, Rozhnov I, Stanimirovic P S, Shkaberina G. Hybrid Algorithms With Alternative Embedded Local Search Schemes For The p-Median Problem. International Journal on Information Technologies & Security, 2023, 15(4):61-72.

[12] Anh A T H T, Duc L H. Super-capacitor energy storage system to recuperate regenerative braking energy in elevator operation of high buildings. International journal of electrical and computer engineering, 2022, 12(2):1358-1367.

[13] Chen Y, Sanz-Alonso D, Willett R. Autodifferentiable ensemble Kalman filters. SIAM Journal on Mathematics of Data Science, 2022, 4(2):801-833.

[14] Potokar E R, Norman K, Mangelson J G. Invariant extended kalman filtering for underwater navigation. IEEE Robotics and Automation Letters, 2021, 6(3):5792-5799.

[15] Wei Y, Zhou B, Zhang J, Sun L, An D, Liu J. Review of Simultaneous Localization and Mapping Technology in the Agricultural Environment. Journal of Beijing Institute of Technology, 2023, 32(3):257-274.

[16] Batuhan G, Serhat K. Multifractal detrended fluctuation analysis of insole pressure sensor data to diagnose vestibular system disorders. Biomedical Engineering Letters, 2023, 13(4):637-648.

[17] Valente N F, Bilro L, Oliveira R. Hydrostatic Pressure Sensor Based on Polymer Optical Fiber Multimode Interferometer. IEEE Sensors Journal, 2023, 23(12):12876-12880.

[18] Chang S, Ji B, Liu L B. Two algorithms of geodesic line length calculation considering elevation in eLoran systems. IET radar, sonar & navigation, 2023, 17(10):1469-1478.

[19] Alam M I, Pasha A A, Jameel A G A, Ahmed U. High altitude airship: A review of thermal analyses and design approaches. Archives of Computational Methods in Engineering, 2023, 30(3):2289-2339.

[20] Svetunkov I, Kourentzes N, Ord J K. Complex exponential smoothing. Naval Research Logistics (NRL), 2022, 69(8):1108-1123.

[21] Hamidy F, Yasin I. Implementation of Moving Average for Forecasting Inventory Data Using CodeIgniter. Journal of Data Science and Information Systems, 2023, 1(1):17-23.

[22] Morales F A, Ramírez J M, Ramos E A. A mathematical assessment of the isolation random forest method for anomaly detection in big data. Mathematical Methods in the Applied Sciences, 2023, 46(1):1156-1177.

[23] Xu H, Pang G, Wang W Y. Deep Isolation Forest for Anomaly Detection. IEEE Transactions on Knowledge and Data Engineering, 2023, 35(12):12591-12604.

[24] Runkai Z, Rong R, John Q. Reliable and fast automatic artifact rejection of Long-Term EEG recordings based on Isolation Forest. Medical and Biological Engineering and Computing: Journal of the International Federation for Medical and Biological Engineering, 2024, 62(2):521-535.